

PCCP

Accepted Manuscript



This is an *Accepted Manuscript*, which has been through the Royal Society of Chemistry peer review process and has been accepted for publication.

Accepted Manuscripts are published online shortly after acceptance, before technical editing, formatting and proof reading. Using this free service, authors can make their results available to the community, in citable form, before we publish the edited article. We will replace this *Accepted Manuscript* with the edited and formatted *Advance Article* as soon as it is available.

You can find more information about *Accepted Manuscripts* in the [Information for Authors](#).

Please note that technical editing may introduce minor changes to the text and/or graphics, which may alter content. The journal's standard [Terms & Conditions](#) and the [Ethical guidelines](#) still apply. In no event shall the Royal Society of Chemistry be held responsible for any errors or omissions in this *Accepted Manuscript* or any consequences arising from the use of any information it contains.

Adsorption of linear aliphatic α,ω -dithiols on plasmonic metal nanoparticles: A structural study based on surface-enhanced Raman spectra

J. Kubackova^{1,2}, I. Izquierdo-Lorenzo¹, D. Jancura^{2,3}, P. Miskovsky^{2,3,4}, S. Sanchez-Cortes¹

¹Instituto de Estructura de la Materia, IEM-CSIC. Serrano 121, 28006 Madrid, Spain

²Department of Biophysics, Faculty of Science, Safarik University, Jesenna 5, 041 54 Kosice, Slovakia

³Center for Interdisciplinary Biosciences, Faculty of Science, Safarik University, Jesenna 5, 041 54 Kosice, Slovakia

⁴International Laser Center, Ilkovicova 3, 812 19 Bratislava, Slovakia

AUTHOR INFORMATION

Corresponding Author

Santiago Sanchez-Cortes. Instituto de Estructura de la Materia (CSIC). Serrano, 121. 28006-Madrid. Spain. E-mail address: s.sanchez.cortes@csic.es

ABSTRACT

The adsorption mechanism of linear aliphatic α,ω -dithiols with chain lengths of 6, 8 and 10 carbon atoms on silver and gold nanoparticles has been studied by surface-enhanced Raman scattering (SERS) spectroscopy. SERS spectra provided the structural marker bands of these compounds which were employed to obtain information about the adsorption and coordination mechanism, the orientation, conformational order, and packing of the aliphatic chains of dithiols on the metal nanoparticles surface. The effect of the type of metal (silver or gold) and the extent of surface coverage on all the above mentioned properties is discussed. It was found that the adsorption of dithiols on Au nanoparticles leads to a more disordered structure of the aliphatic chains of dithiols in comparison with the adsorption on Ag nanoparticles. The interaction through both thiol groups makes the adsorption of dithiols on metal surface substantially different from that of monothiols, in particular the orientation of dithiols is perpendicular, while monothiols adopt a tilted orientation. Dithiols may act as linkers between metal nanoparticles and induce the formation of nanogaps with a controllable interparticle distance. The nanogaps thus formed are able to produce hot spots exhibiting a large intensification of electromagnetic field in these points which has been proved by the observation of intense SERS spectra of dithiols until concentration of 10^{-8} M, corresponding to a large Raman enhancement factor of 5×10^6 .

KEYWORDS: Dithiols, Adsorption, Coordination, Plasmonic nanoparticles, SERS - Surface-enhanced Raman scattering,

INTRODUCTION

The interest for plasmonic metal nanoparticles (NPs) has grown in the last years due to the large list of their applications in many fields such as environment, medicine, chemistry and optics. These applications are possible thanks to the great potential of NPs in chemical detection, clinical diagnosis, heterogeneous catalysis, and many other areas¹⁻³. The potential of NPs is related to the localized surface plasmon resonances (LSPR) induced on the surface of NPs giving rise to a strong enhancement of the electromagnetic (EM) field in the vicinity of these nanoparticles⁴. This phenomenon also enables the application of NPs in optical spectroscopy, particularly the surface-enhanced Raman scattering (SERS) technique. Spherical NPs (SNP) were previously employed to reach large intensifications of the Raman signal by SERS⁵. However, the SERS enhancement in colloidal SNPs suspensions can be substantially increased by the aggregation of SNPs, specially by the controlled link of nanoparticles, since a huge intensification of the electromagnetic (EM) field can be induced in interparticle gaps or nanogaps (NGs)⁶. In fact, these NGs are also called hot spots (HS) due to this large EM intensification. The formation of size-controlled NGs between plasmonic surfaces has given rise to an extensive research, both theoretical and experimental⁷⁻¹². The controlled aggregation of NPs is a key process to induce the formation of *hot spots* and to obtain a high intensity Raman signal from the analysed molecules. A better control of the NPs linking can be achieved by using bifunctional molecular linkers. These systems provide a double advantage in comparison with other aggregating agents: i) the formation of interparticle gaps with dimensions determined by the structural properties of the linker, and ii) the modification of the NPs surface properties by molecular functionalization, which may induce the localization of the molecular analyte just in the NGs created by the linker. The last feature makes possible the assembly of other substances

otherwise showing no affinity towards the metal surface. In previous studies several bifunctional molecular linkers have been successfully employed in the creation of NGs of controllable sizes, providing a suitable chemical environment to stimulate the hosting of analytes with a high sensitivity and selectivity¹³⁻²¹. In this regard, viologen dications and α,ω -diamines have been used in the functionalization of silver nanoparticles and have been proven to be suitable systems for the detection of pollutants and pesticides by the formation of interparticle cavities where analysed molecules are hosted^{18, 19, 22}. Dithiol-containing molecules have been also employed as NPs linkers by Moskovits *et al.*^{14, 23}, demonstrating that NPs-dithiol system can be also very effective systems for SERS experiments. In our previous work we have tested the ability of dithiols to bind silver nanoparticles, as well as the effect of the adsorption of these bifunctional molecules on the NPs linking and the hot spot creation²⁴. In continuation of this work we present a study of the adsorption of several types of linear aliphatic α,ω -dithiols (DTX), having 6, 8 and 10 carbon atoms in their chain (Figure 1), on plasmonic NPs of different nature.

The adsorption of dithiols on metal surfaces was previously studied by RAIRS vibrational spectroscopy²⁵⁻²⁸, but Raman spectroscopy has not been employed so far to characterize the self-assembly of these important molecules on metals. However, the adsorption of related monothiols on metal surfaces was extensively studied in recent years also by Raman spectroscopy²⁹⁻³³. Highly packed self-assembled monolayers formed from 1-thiols were studied by Bryant and Pemberton using SERS³⁴, but the growth mechanism of these layers by conformational analysis in the sub-monolayer regime is reported here for the first time thanks to the high sensitivity of SERS from molecules placed in highly sensitive nanogaps.

The present work is mainly focused on the study of the adsorption of dithiols on metal surface by analysing key structural SERS spectral markers of the adsorption, metal coordination,

orientation, ordering and interfacial packing of these molecules on surfaces of silver and gold NPs. The fingerprint character of SERS spectra, the propensity rules of SERS³⁵ and the high sensitivity of this technique makes this study possible even at the very low concentration of dithiols. SERS is the unique technique that can afford structural information about dithiols at the very low coverage surfaces analysed in this work (nanomolar level), due to its high sensitivity, and specifically from the molecules allocated in NGs. The information obtained from this study can provide a better understanding of the adsorption process of alkene dithiols on plasmonic metal nanoparticles, with the potential to get more insight in the immobilization, interparticle linking and nanocontact experiments where these important molecules are involved³⁶⁻⁴⁰.

EXPERIMENTAL METHODS

1,6-hexanedithiol (DT6) was purchased from Sigma Aldrich, while 1,8-octanedithiol (DT8) and 1,10-decanedithiol (DT10) were obtained from Alfa Aesar. Stock solutions of these substances were prepared in ethanol at 0.1 M concentration and were further diluted when necessary.

Au NPs in colloidal suspension prepared by reduction with citrate (AuC) were prepared by using the method described by Sutherland and Winefordner³⁶. Briefly, 0.1 mL of an aqueous solution of HAuCl₄ (0.118 M) was diluted in 40 mL of water, under intense stirring. 1 mL of 1% sodium citrate solution in volume was added dropwise. The yellow solution was refluxed for 5 minutes, resulting in a red colloidal suspension. The average diameter of Au nanoparticles prepared by the above method is 20 nm⁴¹.

Ag NPs in suspension were prepared by two different methods. Citrate Ag NPs (AgC) were obtained by the following procedure⁴²: a total of 1 mL of a 1% (w/v) trisodium citrate aqueous

solution was added to 50 mL of a boiling 10^{-3} M silver nitrate aqueous solution, and boiling was continued for 1 h. The obtained colloid showed a turbid gray aspect and had a final pH of 6.5. Hydroxylamine Ag NPs (AgH) were obtained by the method described previously by Cañamares et al.⁴² Briefly, 10 mL of a 10^{-2} M silver nitrate solution are added dropwise to 90 mL of a 1.6×10^{-3} M solution of hydroxylamine hydrochloride adjusted to pH=9 under vigorous stirring. The resulting spherical Ag NPs have an average size of 35 nm in diameter⁴².

Raman and SERS spectra were registered using a Renishaw InVia instrument equipped with an electrically refrigerated CCD camera and a Leica DM 2500 microscope. The 532 nm line provided by a Nd-YAG laser (Samba model, Cobolt) and the line at 785 nm provided from a diode laser (HPNIR 785 model, Renishaw) were used as excitation sources. An UV-visible-NIR Shimadzu 3600 spectrometer equipped with a PMT for light detection in the UV-visible range and an InGaAs detector for the NIR was employed to obtain the plasmon extinction spectra.

Transmission electron microscopy images were taken using a JEOL JEM-2010 with an acceleration voltage of 200 kV.

RESULTS AND DISCUSSION

Extinction spectra of NPs in the presence of dithiols

The effect of dithiols on the plasmon resonance of NPs was studied at several dithiol concentrations. Since this investigation was systematically developed in our previous work²⁴, we display here only the study carried out at different DT8 concentrations (Figure 2). In the absence of a linker, the extinction spectrum of the colloid exhibits the usual profile consisting of a narrow Lorentzian band with a maximum at 406 nm corresponding to isolated NPs (Figure 2a and inset TEM images). At concentrations above 10^{-6} M, large changes in the extinction spectra are observed due to the strong NPs assembly induced by DT8. The main effect is the intensity

decrease of the band at 413 nm, corresponding to 406 nm band of the unaggregated NPs, and the appearance of a wide band centred approximately at 800 nm (observed at 5×10^{-6} M concentration of DT8, Figure 2b). The threshold concentration for the induction of this band in the NPs suspension is the same for all the investigated dithiols and corresponds to the concentration (1-5 μM) at which a full surface coverage is reached as shown below. This indicates that the aggregation is a consequence of the full surface coverage induced by the linking of DTX to NPs, which occurs at approximately the same threshold concentration for all the studied linkers. Thus, the strong change observed in the absorption spectra of the aggregated Ag NPs is attributed to the complete surface coverage expected at the a concentration above 1 μM . DT8 induces the formation of aggregates having a chain-like morphology as indicated in the inset graph of Figure 2b. In these chains the nanoparticles are distributed in such a manner that the average distance between the neighbouring NPs oscillates between 1 and 2 nm, as deduced from the TEM micrographs²⁴.

The appearance of an intense extinction band at 565-575 nm (Figure 2c) at high DT8 concentration (50 μM) is attributed to the formation of dense globular aggregates as indicated in the inset TEM images. This kind of aggregation is more evident in the case of DT8 and DT10 in comparison with DT6 (not shown).

SERS Spectra of dithiols

Figures 3-5 show the SERS spectra of DT6, DT8 and DT10 obtained on AgH. SERS spectra of dithiols obtained on AgC are very similar to the spectra obtained using AgH colloid, but also display strong citrate features at DTX concentrations below 1 μM (not shown). In contrast, the SERS spectra registered on AuC display different profiles as shown in Figure 6b and c. Intense SERS spectra were obtained until a very low concentration of dithiols (10^{-8} M), in spite of the

low Raman cross section of these compounds. This high sensitivity indicates that dithiols are effectively forming hot spots where the EM field is highly enhanced and consequently the Raman signal of these molecules is substantially enhanced. The SERS enhancement factor for DT8 at concentration of 10^{-8} M was determined to be 5×10^6 , demonstrating that this enhancement is actually strong and comparable to those typical for very active SERS molecules such as dyes and aromatic compounds.

The assignment of the vibrational bands of the adsorbed dithiols was made on the basis of the data found in the literature^{14, 31}. Table 1S (Supporting Information) presents the positions of the main bands observed in SERS spectra as well as their assignments.

SERS spectra reveal that dithiols interact strongly with plasmonic metals via the formation of a covalent bond through both S atoms and the formation of alkanedithiolate species. This is deduced from the disappearance of the strong S-H stretching band at 2570 cm^{-1} seen in neat liquid dithiols (Figure 3-5a). Alkane monothiols also show a similar behaviour when adsorbed on metals³⁶. SERS spectra provide an additional hint of this interaction since the bands appearing at 220 cm^{-1} , in the case of AgH (Figure 6d), and at 280 and 170 cm^{-1} in AuC (Figure 6c). These bands can be assigned to stretching vibrations of the Ag-S and Au-S bonds formed upon dithiol adsorption on metal surface^{32, 43, 44}. The presence of two Au-S bands indicate that the thiol groups are interacting with the metal surface through two different coordination mechanisms. Miao et al. reported the existence of three adsorption sites on Au: top, bridge and hollow⁴⁵. Therefore, we suggest that the appearance of these two Au-S bands is due to the existence of two coordination mechanisms of the adsorbed molecules on the gold surface as also reported by Kato et al.³² In fact, the relative intensity of the higher wavenumber component rises upon increasing the concentration of dithiols, due to the increasing importance of the on-top coordination

mechanism at high coverage conditions. The presence of only one Ag-S band at 220 cm^{-1} may indicate that the coordination of sulfur atom with Ag occurs through only one coordination mechanism.

The complete disappearance of the band corresponding to SH bond indicate that both SH groups interact with the metal and consequently the SERS signal corresponds mainly to dithiol molecules linked to NPs and placed in nanogaps. This is expected to be valid predominantly at low surface coverage. Molecules localized out of these gaps could also contribute to the SERS spectra but undergoing a much lower intensification as deduced from the absence of free SH bands. Nevertheless, this effect could be also related to the possible lying-down (LD) orientation of dithiols on the metal surface²⁵ as shown in Figure 7A. In the next sections we analyse the SERS spectra of DTX on Ag and Au NPs separately.

SERS of dithiols on AgNPs

In liquid state of DTX, a strong $\nu_G(\text{C-S})$ band appearing at $660\text{-}650\text{ cm}^{-1}$ in the Raman spectra indicates a high molecular disorder of DTX molecules (Figures 3a-5a). When dithiols are adsorbed onto the metal surface, two SERS bands appear at approximately 700 and 630 cm^{-1} , corresponding to the $\nu_T(\text{C-S})$ (T=*trans*) and $\nu_G(\text{C-S})$ (G=*gauche*) bands, respectively^{24, 29}. Comparing the Raman spectra of neat liquid dithiols with the SERS ones (Figures 3-5), a relative intensification of the $\nu(\text{C-S})$ bands is observed in comparison with the bands corresponding to the $\nu(\text{CH})$ and $\delta(\text{CH}_2)$ vibrations of the aliphatic central moiety. This effect is more evident for DT6 (Figure 3), where less CH_2 groups are present in the aliphatic chain. Additionally, the degree of structural order in the aliphatic chain or crystallinity of dithiols molecules^{24, 46} can be followed by analyzing the ratio $R_{CS}=I_{CST}/I_{CSG}$ of $\nu(\text{C-S})$ bands. Figure 8A shows the R_{CS} values determined when varying the chain length and the surface coverage related to the different

molecular self-assembly. While DT6 exhibits a highly disordered structure on the surface at all the studied concentrations, DT10 shows a more ordered structure in comparison to the liquid sample. It is worth noting that the DT10 displays a remarkable increase of the R_{CS} value at concentrations above 8×10^{-6} M. Finally, DT8 display an intermediate behavior with a significant increase of R_{CS} at concentrations above 10^{-5} M, but with R_{CS} values closer to DT6 at very low concentrations ($<10^{-7}$ M). These data indicate that the conformational order of the methylene groups close to the CS group in DTX increases at high surface coverage due to a tighter molecular packing.

The adsorption of dithiols on the metal surface also induces a strong downshift of $\nu(\text{C-S})$ wavenumber in relation to the position of the same band in neat liquid samples. This effect was also observed by Bryant et al. in the case of monothiols, and was attributed to the strong withdrawal of electrons from C-S bond in the interaction with the metal³⁴. The downshift extent depends on the surface coverage and the nature of the metal, being more pronounced at low coverage and when dithiols are adsorbed on Ag. It was reported that the extent of this shift increases with the number of metal atoms involved in the bond⁴³, due to the fact that the coordination *via* hollow sites involves a higher π contribution, which is in turn antibonding with respect to the S-C bond⁴⁷. Thus, the large downshift observed for dithiols adsorbed on Ag NPs suggests that the coordination of the thiolate group to the Ag surface takes place through hollow sites, and that coordination is related to the appearance of the $\nu(\text{Ag-S})$ band at 220 cm^{-1} . This coordination was also proposed by Cho et al. for the adsorption of thiols on Ag electrodes⁴³.

As the concentration of DTX is raised, the probability of interaction of these molecules with one or two metal atoms (on-top and bridge coordination) increases, and this accounts for the lower red shift of the $\nu(\text{C-S})$ frequency at higher coverage. Furthermore, another factor that can

influence the position of the C-S stretching is the strong withdrawing capacity of residual chloride ions, coming from the preparation process of AgH, that are still adsorbed onto the metal surface at low dithiol concentrations, as reveals the presence of an intense band at 235 cm^{-1} attributed to $\nu(\text{Ag-Cl})$ (result not shown).

The conformational changes occurring on varying the surface coverage are also manifested in the C-H stretching region. In liquid dithiols two main bands in this region appear at ca. 2925 and 2850 cm^{-1} (Figures 3-5a). The first one can be attributed to an overtone of CH_2 bending in Fermi resonance with $\nu_{\text{as}}(\text{CH}_2)$ vibration, while the latter band is attributed to $\nu_{\text{s}}(\text{CH}_2)$ ⁴⁸. In addition, a shoulder can be seen at 2898 cm^{-1} and this is assigned to the $\nu_{\text{as}}(\text{CH}_2)$ vibration. This spectral profile is typical for melted polymethylene chains, where the chain adopts a highly disordered structure⁴⁹. The ratio R_{CH} (I_{2930}/I_{2850}) is connected to the content of G conformers relative to the T ones in polymethylene chains⁴⁸. In dithiols, the absence of terminal CH_3 groups facilitates the study of the order based on the R_{CH} ratio as no overlapping from the $\nu_{\text{s}}(\text{CH}_3)$ vibration is expected in this case in contrast to what happens in monothiols^{50, 51}. In neat liquids, R_{CH} decreases from DT6 to DT10 indicating an increase of the chain order. In this context, the intensity increase of the band at 2898 cm^{-1} in dithiols of longer chain has been attributed to an increase of the lateral packing according to Wong et al⁵².

The adsorption of DTX on Ag surface leads to important changes in the C-H region as compared to neat liquid samples. By one hand, an intensity decrease of the C-H bands in relation to the CC/CS bands is observed, thus suggesting a dominant perpendicular orientation of the main molecular axis of dithiols on the surface. On the other hand, an increase of the molecular packing upon adsorption can be deduced from the relative enhancement of the $\nu_{\text{as}}(\text{CH}_2)$ band at 2898 cm^{-1} , mostly seen in DT6 (Figure 3), and as also reported previously by other authors⁵²⁻⁵⁴.

The intensification of the 2898 cm^{-1} band avoids a proper analysis of the R_{CH} ratio due to its overlapping with the other two CH bands. However, the high intermolecular interaction derived from the tight molecular packing seems to induce an increase of the conformational order and the molecular packing of aliphatic chains, as deduced from the shift downward of the 2925 cm^{-1} band, suggesting an increase of T conformers in the chain^{49, 55}. This deduction suggest a well organised self-assembled monolayer (SAM) of dithiols on the surface, involving a more ordered structure⁵⁶. The 2850 cm^{-1} band is enhanced when the surface coverage is high and as the length of the polymethylene is raised, indicating that the conformational order also increases at the latter conditions due to the existence of better conditions for the establishment of well-organized SAM as depicted in Figure 7B.

The analysis of the C-C stretching region ($1150\text{-}1000\text{ cm}^{-1}$) also reveals important information concerning the conformational order of the aliphatic chain in dithiols. As in the case of the C-S stretching, the bands corresponding to both T and G conformers can be found in the Raman spectra ($\nu_{\text{T}}(\text{C-C})$ and $\nu_{\text{G}}(\text{C-C})$). The Raman spectra of liquid DTX display a medium intensity band at $1085\text{-}1070\text{ cm}^{-1}$ which can be attributed to $\nu_{\text{G}}(\text{C-C})$ ³⁴. The adsorption of dithiols on Ag leads to changes in this region depending on the aliphatic chain length and the concentration. The SERS spectral profile of DT6 does not change significantly in comparison to Raman spectrum of this dithiol in the neat sample (Figure 3). This suggests the formation of a rather disordered layer of DT6 on the Ag surface, which is in agreement with the analysis of the $\nu(\text{C-S})$ bands. In the case of DT8, the intensification of two narrow $\nu(\text{C-C})$ bands at 1084 and 1011 cm^{-1} is observed at high concentration (above $5 \times 10^{-5}\text{ M}$, Figure 4b), which is related to the increase of the chain conformational order. These two bands may correspond to the $\nu_{\text{T}}(\text{C-C})$ bands appearing at $1113/1090$ and 1050 cm^{-1} in octadecanethiol adsorbed onto Ag^{14, 34}. The fact that these two

bands are shifted toward lower wavenumber values is probably due to the simultaneous linking of the dithiol with two Ag surfaces, what may induce a change in the vibration frequency of C-C bonds placed between two Ag nanoparticles.

The orientation of the main molecular axis of DTX related to the metal surface can be estimated from SERS spectra by considering the SERS propensity selection rules, which predict a higher intensification of vibrational modes perpendicular to the surface^{35, 57}. The stretching vibrations of DTX can be used to carry out the orientation study because they imply variations of the tensor component along the axis of a vibration. In addition, $\nu(\text{C-S})$ and $\nu(\text{C-C})$ modes are orthogonal to the $\nu(\text{C-H})$ ones, and will be differently enhanced when the molecule is adsorbed on a surface in comparison to the relative intensities of Raman bands of neat liquid samples³⁴. Thus, the $\nu(\text{C-S})/\nu(\text{C-H})$ or $\nu(\text{C-C})/\nu(\text{C-H})$ ratios ($I_{\text{CS}}/I_{\text{CH}}$ and $I_{\text{CC}}/I_{\text{CH}}$), where I_{CS} , I_{CH} and I_{CC} represents the integrated intensity of all the bands of the same type, can be used to estimate the orientation of the main axis of dithiols on the surface³⁴. We have used the ($I_{\text{CC}}/I_{\text{CH}}$) ratio to monitor the molecular orientation of dithiols, by normalizing this parameter to the same ratio of the neat liquid sample ($I_{\text{CC}}^0/I_{\text{CH}}^0$). This ratio represents in a better way the orientation of the molecular chain in contrast to the $I_{\text{CS}}/I_{\text{CH}}$ one, which is rather related to the CS environment. To accomplish this procedure we have employed the spectra recorded with an excitation line at 532 nm, since a higher signal-to-noise ratio was obtained in the CH stretching region at this excitation. Figure 8B shows the plot of the $[(I_{\text{CC}}/I_{\text{CH}})/(I_{\text{CC}}^0/I_{\text{CH}}^0)]$ ratio (R) calculated from SERS and Raman spectra of DTX at different concentrations. As can be seen, R increases significantly at concentrations above a threshold concentration of 5×10^{-6} M reaching a value of 13 and 10.5 in the case of DT10 and DT8, respectively, meaning that the orientation of DTX on Ag surface is predominantly perpendicular at concentrations above this threshold value. This finding indicates

that these dithiols adopts a standing-up orientation above the threshold concentration. The decrease of this ratio at lower concentrations is rather attributable to a lowering of the conformational order of the aliphatic chain which can eventually give rise to lying-down structures. From the values of R obtained at high surface coverage (above 10^{-5} M), at which an all-*trans* conformational structure is expected, one can also calculate the tilt angle of the chain in relation to the surface (see Supporting Information for more details). The estimated tilt angle in the case of DT10 and DT8 is less than ca 5° (Table 2S) with respect to the surface normal. This indicates that the orientation of the aliphatic chain is almost perpendicular in contrast to the results obtained for monothiols³⁶. The differences found between dithiols and monothiol can be attributed to the existence of two terminal thiol groups in DTX molecules, which are the responsible for the behaviour regarding the tilt angle and the interchain packing.

In the case of DT6 a higher tilt angle ($8-10^\circ$, Table 2S) was deduced, but this is again associated to a lower conformational order in the aliphatic chain of DT6. This lower order also induces an enhancement of the bands attributed to the twisting vibrational modes of CH_2 appearing in the $1250-1150\text{ cm}^{-1}$ regions. However, in the case of DT8 the enhancement of twisting bands and the $\nu_{\text{C-S}}$ band is mainly observed at submonolayer concentration ($<10^{-7}$ M), thus suggesting that a lying-down orientation is possible at low surface coverage (Figure 7A). This orientation is also highly probable in DT6, even at concentrations above the SAM conditions, as the structural order is very low for this dithiol at all the investigated concentrations.

At a high surface coverage, a band corresponding to the vibration of free S-H groups appears at ca. 2570 cm^{-1} (Figure 3-5b). The appearance of this band suggests that DTX molecules start to self-assemble inside nanogaps, forming multilayered structures where the free S-H groups may

be present (Figure 7C). Figure 9A displays the intensity of $\nu(\text{S-H})$ band (I_{SH}) vs. the dithiol concentration for the three studied dithiol molecules on AgH NPs. The intensity of the $\nu(\text{S-H})$ band increases substantially at concentrations above $1 \mu\text{M}$, probably due to the saturation of the metal surface inside interparticle spaces and the formation of multilayers. The SERS intensity of free $\nu(\text{S-H})$ band measured at a fixed dithiol concentration is higher as the alkylic chain of DTX is longer. This observation is attributed to the stronger intermolecular interaction existing in the longer chains, i.e. DT8 and DT10, that are more suitable to form multi-layered structures adsorbed onto Ag. The appearance of the free S-H band is also associated to the presence of $\nu(\text{C-S})$ bands corresponding to free C-SH groups, observed at the same wavenumber values as in the liquid dithiol.

The $\nu(\text{S-H})$ band in SERS spectra of dithiols was used to study the adsorption of these adsorbates onto different metallic platforms. The concentration dependence of the intensity of $\nu(\text{S-H})$ band of DT8 adsorbed on the different substrates employed in this work, AgH, AgC, AuC, is shown in Figure 9B. In all cases an increase of the intensity of this band is observed above a concentration $1 \mu\text{M}$, but the growth is steeper in the case of Au in relation to Ag nanoparticles. This fact can be explained by two different effects: i) the lower available surface existing in Au NPs as compared to that of Ag NPs⁴¹, while AgH and AgC show a similar available adsorption surface and ii) the different adsorption and coordination mechanism of dithiols on Au in comparison with Ag nanoparticles.

SERS on Au colloid

SERS spectra of DTX on AuC were also recorded at different concentrations. As an example we show the SERS spectra of DT8 registered at two concentrations: $8 \times 10^{-6} \text{ M}$ and 10^{-4} M (Figure 6b and c). The lower downshift undergone by the $\nu(\text{C-S})$ bands on this metal in comparison to

Ag NPs suggests a weaker interaction of DTX with Au surface. Shifts from 737 to 703 cm^{-1} and from 655 to 640 cm^{-1} for $\nu_{\text{T}}(\text{C-S})$ and $\nu_{\text{G}}(\text{C-S})$, respectively, were observed in the SERS spectra on Au NPs. The weaker interaction is also related to the appearance of the $\nu(\text{Au-S})$ band at 280 cm^{-1} , which is attributed to the on-top coordination of S atoms on Au surface, provided that this coordination mechanism is energetically less favourable than the three-fold hollow or two-fold bridge coordinations⁵⁸. This kind of coordination was reported to occur in the adsorption of aliphatic thiols on Au⁴³. On the other hand, the weak band at 220 cm^{-1} is attributed to the $\nu(\text{Au-S})$ of dithiol linked to bridge or hollow sites.

The SERS of DT8 on AuC at low concentrations (Figure 6b) resembles the Raman spectrum of this dithiol in the liquid state (Figure 6a), except for the $\nu(\text{C-S})$ bands, which are weaker, and the bands at 1300 cm^{-1} (attributed to $\omega(\text{CH}_2)$) and those appearing in the 910-875 cm^{-1} region attributed to $\rho(\text{CH}_2)$, which are relatively stronger in the SERS spectrum. At concentrations higher than 1 μM , which represents the concentration needed for the saturation of the metal surface covering by dithiols, the bands corresponding to free SH groups are stronger than in Ag colloids. The appearance of the free SH band is also accompanied by an intensity increase of $\nu_{\text{T}}(\text{C-S})$ and $\nu_{\text{G}}(\text{C-S})$ bands of free CSH groups at 737 and 655 cm^{-1} , respectively, at concentration 10^{-4} M.

The high similarity between the SERS spectrum of dithiols adsorbed on Au and the Raman spectrum of the neat liquid sample points out the existence of a more disordered structure of DTX on Au than on Ag NPs. Indeed, this conclusion is also supported by the appearance of a strong band at 1081 cm^{-1} corresponding to $\nu_{\text{G}}(\text{C-C})$ ³⁴.

Regarding the orientation of dithiols on AuC, the lower intensity of $\nu(\text{C-S})$ bands in relation to the SERS spectrum of DT8 on Ag at the same concentration (Figure 6d) suggests a less

perpendicular orientation of the C-S bond with respect to the Au surface than in the case of Ag. A similar result was reported by Bryant et al.³⁴ for monothiols. This orientation seems to be related to the coordination of DTX through on-top sites, since this mechanism implies a more tilted orientation associated to the sp^3 hybridization of the S atom⁴⁷.

As in the case of Ag NPs, the intensification of the bands corresponding to $\nu(\text{C-C})$ and $\nu(\text{C-S})$ vibrations with increasing the dithiol concentration indicates that the aliphatic chains re-orientate towards a more perpendicular orientation.

CONCLUSIONS

In this work we have demonstrated that SERS is a very useful tool to get information about the adsorption of dithiols on plasmonic metal NPs also at very low molecular concentrations. Intense SERS spectra were obtained until a 10^{-8} M concentration of dithiols, corresponding to a large enhancement factor (5×10^6). These observations demonstrates that the dithiols are placed in interparticle gaps forming hot spots where the EM field and Raman signal are highly enhanced.

The analysis of the metal-DTX stretching vibrations demonstrates that the coordination of dithiols is different on the studied metals, being the bond with Ag more stable due to the interaction with hollow sites, while in the case of Au surface, dithiols seem to interact through different sites, although top sites are the most probable.

The conformation and molecular packing of adsorbed dithiols is highly determined by the extent of the surface coverage of plasmonic nanoparticles. The spectral changes are not continuous and there is a threshold concentration at which drastic variations in the adsorption mechanism and the structure of the dithiols are observed. This threshold dithiol concentration is ca. $1\mu\text{M}$. The structural vibrational markers deduced from the SERS spectra (SH, CC, CS and CH stretching bands) suggest that there are three main pictures that emerge from the analysis of

the adsorption of these molecules on metal surfaces. At concentrations below the threshold value both thiol groups are attached to the metal surface forming nanogaps, where the SERS intensification should be very high. At concentrations in the range of 1-5 μM , the full surface coverage leads to the formation of a dithiol SAM characterized by a significant increase of the aliphatic chain order, particularly in DT10 and DT8. Above the threshold concentration dithiols are organized in multi-layered structure giving rise to a nanoparticle separation which is detected in the plasmon extinction spectra. The study of the order/disorder indicates that the adsorbed DT6 bears a very disordered structure for all the studied concentrations, whereas DT10 is highly ordered, even at lower concentrations, due to the longer aliphatic chain, which favors the formation of intermolecular interactions for all the studied concentrations. DT8 undergoes an intermediate behavior showing a transition from a disordered structure at concentrations below 1 μM to an ordered one at above this threshold concentration. Moreover, we have found that the adsorption of dithiols on Au nanoparticles leads to a more disordered structure of the aliphatic chains of DTX in comparison with the adsorption on Ag NPs.

The orientation of the aliphatic chains is almost perpendicular at high concentrations, in contrast to the results obtained for monothiols⁵⁹. This difference is attributed to the bifunctional character of dithiols, which behaviour differs from that of monothiols regarding the tilt angle and the interchain packing. The orientation of DTX on Au is more tilted as suggests the low intensity of CS stretching vibrations. These findings together with the different coordination deduced for dithiols on Ag and Au surfaces demonstrate that a significant difference exists between these plasmonic metals in the interaction with thiols. This effect must indeed be considered in functionalization processes where dithiols molecules are employed.

ACKNOWLEDGMENTS

This work has been supported by the Spanish *Ministerio de Economía y Competitividad* (MINECO, grant FIS2010-15405) and *Comunidad de Madrid* through MICROSERES II network (grant S2009/TIC-1476), by the Agency of the Ministry of Education of Slovak Republic for the Structural funds of the European Union, Operational program Education (Doctorand, ITMS code: 26110230013 and KVARK, ITMS code: 26110230084) and Operational program Research and Development (NanoBioSens (ITMS code: 26220220107) and CEVA II (ITMS code: 26220120040)), by the Slovak Research and Development Agency under the contract APVV-0242-11, and by the project CELIM (316310) funded by 7FP EU.

Supplementary Information: Table with the wavenumbers and assignments of the main bands observed in Raman and SERS spectra of DT8 (Tab S1). Calculation of tilt angles of dithiols adsorbed on Ag and Au (the used metal) NPs (Tab S2).

References

1. M. A. El-Sayed, *Accounts Chem Res*, 2004, 37, 326-333.
2. J. N. Anker, W. P. Hall, O. Lyandres, N. C. Shah, J. Zhao and R. P. Van Duyne, *Nat Mater*, 2008, 7, 442-453.
3. M. Schütz, D. Steinigeweg, M. Salehi, K. Kömpe and S. Schlücker, *Chem Comm*, 2011, 47, 4216-4218.
4. R. Aroca, *Surface-enhanced Vibrational Spectroscopy*, John Wiley & Sons Chichester 2006.
5. J. A. Creighton, C. G. Blatchford and M. G. Albrecht, *J Chem Soc Farad T2*, 1979, 75, 790-798.
6. M. Futamata, *Faraday Discuss*, 2006, 132, 45-61.
7. W. Y. Li, P. H. C. Camargo, X. M. Lu and Y. N. Xia, *Nano Lett*, 2009, 9, 485-490.
8. M. M. Xu, M. Wang, J. L. Yao, W. J. Zou, L. Ling and R. A. Gu, *Spectrosc Spect Anal*, 2009, 29, 1289-1291.
9. C. L. Du, M. X. Yang, Y. M. You, T. Chen, H. Y. Chen and Z. X. Shen, *Chem Phys Lett*, 2009, 473, 317-320.
10. M. Rycenga, P. H. C. Camargo and Y. N. Xia, *Soft Matter*, 2009, 5, 1129-1136.
11. P. H. C. Camargo, M. Rycenga, L. Au and Y. N. Xia, *Angew Chem Inter Ed*, 2009, 48, 2180-2184.
12. J. Zuloaga, E. Prodan and P. Nordlander, *Nano Lett*, 2009, 9, 887-891.
13. J. M. Romo-Herrera, R. A. Alvarez-Puebla and L. M. Liz-Marzan, *Nanoscale*, 2011, 3, 1304-1315.
14. D. J. Anderson and M. Moskovits, *J Phys Chem B*, 2006, 110, 13722-13727.
15. J. I. L. Chen, Y. Chen and D. S. Ginger, *J Am Chem Soc*, 2010, 132, 9600-9601.
16. L. Guerrini, A. E. Aliaga, J. Carcamo, J. S. Gomez-Jeria, S. Sanchez-Cortes, M. M. Campos-Vallette and J. V. Garcia-Ramos, *Anal Chim Acta*, 2008, 624, 286-293.
17. L. Guerrini, J. V. Garcia-Ramos, C. Domingo and S. Sanchez-Cortes, *J Phys Chem C*, 2008, 112, 7527-7530.
18. L. Guerrini, J. V. Garcia-Ramos, C. Domingo and S. Sanchez-Cortes, *Anal Chem*, 2009, 81, 1418-1425.
19. L. Guerrini, I. Izquierdo-Lorenzo, J. V. Garcia-Ramos, C. Domingo and S. Sanchez-Cortes, *Phys Chem Chem Phys*, 2009, 11, 7363-7371.
20. E. C. Cho, S. W. Choi, P. H. C. Camargo and Y. Xia, *Langmuir*, 2010, 26, 10005-10012.
21. P. Pramod and K. G. Thomas, *Adv Mater*, 2008, 20, 4300-4305.
22. L. Guerrini, I. Izquierdo-Lorenzo, R. Rodriguez-Oliveros, J. A. Sanchez-Gil, S. Sanchez-Cortes, J. V. Garcia-Ramos and C. Domingo, *Plasmonics*, 2009, 5, 273-286.
23. S. J. Lee, A. R. Morrill and M. Moskovits, *J Am Chem Soc*, 2006, 128.
24. I. Izquierdo-Lorenzo, J. Kubackova, D. Manchon, A. Mosset, E. Cottancin and S. Sanchez-Cortes, *J Phys Chem C*, 2013, 117, 16203-16212.
25. P. Carro, A. H. Creus, A. Munoz and R. C. Salvarezza, *Langmuir*, 2010, 26, 9589-9595.
26. V. S. Dilimon, J. Denayer, J. Delhalle and Z. Mekhalif, *Langmuir*, 2012, 28, 6857-6865.
27. H. He, Y. Guo, S. F. Wang and Y. Q. Jiang, *Surf Rev Lett*, 2010, 17, 397-403.

28. M. A. Daza Millone, H. Hamoudi, L. Rodriguez, A. Rubert, G. A. Benitez, M. Elena Vela, R. C. Salvarezza, J. Esteban Gayone, E. A. Sanchez, O. Grizzi, C. Dablemont and V. A. Esaulov, *Langmuir*, 2009, 25, 12945-12953.
29. T. H. Joo, K. Kim and M. S. Kim, *J Mol Struct*, 1987, 158, 265-274.
30. T. Kasahara, H. Shinohara, Y. Oshima, K. Kadokura, Y. Uriu, C. Ohe and K. Itoh, *Surf Sci*, 2004, 558, 65-79.
31. N. Sandhyarani and T. Pradeep, *Vacuum*, 1998, 49, 279-284.
32. H. S. Kato, J. Noh, M. Hara and M. Kawai, *J Phys Chem B*, 2002, 106, 9655-9658.
33. J. Noh, H. S. Kato, M. Kawai and M. Hara, *J Phys Chem B*, 2006, 110, 2793-2797.
34. M. A. Bryant and J. E. Pemberton, *J Am Chem Soc*, 1991, 113, 3629-3637.
35. M. Moskovits, *J Chem Phys*, 1982, 77, 4408-4416.
36. L. H. Dubois and R. G. Nuzzo, *Ann Rev Phys Chem*, 1992, 43, 437-463.
37. Y. Fu, P. Li, L. Bu, T. Wang, Q. Xie, J. Chen and S. Yao, *Anal Chem*, 2011, 83, 6511-6517.
38. H.-B. He, B. Li, J.-P. Dong, Y.-Y. Lei, T.-L. Wang, Q.-W. Yu, Y.-Q. Feng and Y.-B. Sun, *ACS Appl Mater Interfaces*, 2013, 5, 8058-8066.
39. J. Tournébizé, A. Boudier, A. Sapin-Minet, P. Maincent, P. Leroy and R. Schneider, *ACS Appl Mater Interfaces*, 2012, 4, 5790-5799.
40. X. D. Cui, A. Primak, X. Zarate, J. Tomfohr, O. F. Sankey, A. L. Moore, T. A. Moore, D. Gust, G. Harris and S. M. Lindsay, *Science*, 2001, 294, 571-574.
41. I. Izquierdo-Lorenzo, I. Alda, S. Sanchez-Cortes and J. V. Garcia-Ramos, *Langmuir*, 2012, 28, 8891-8901.
42. M. V. Canamares, J. V. Garcia-Ramos, J. D. Gomez-Varga, C. Domingo and S. Sanchez-Cortes, *Langmuir*, 2005, 21, 8546-8553.
43. S. I. Cho, E. S. Park, K. Kim and M. S. Kim, *J Mol Struct*, 1999, 479, 83-92.
44. G. J. Kluth, C. Carraro and R. Maboudian, *Phys Rev B*, 1999, 59, R10449-R10452.
45. L. Miao and J. M. Seminario, *J Chem Phys*, 2007, 126, 184706.
46. M. A. Bryant and J. E. Pemberton, *J Am Chem Soc*, 1991, 113, 8284-8293.
47. H. Sellers, A. Ulman, Y. Shnidman and J. E. Eilers, *J Am Chem Soc*, 1993, 115, 9389-9401.
48. S. Abbate, G. Zerbi and S. L. Wunder, *J Phys Chem*, 1982, 86, 3140-3149.
49. S. Abbate, S. L. Wunder and G. Zerbi, *J Phys Chem*, 1984, 88, 593-600.
50. R. G. Snyder, H. L. Strauss and C. A. Elliger, *J Phys Chem*, 1982, 86, 5145-5150.
51. R. G. Snyder, *J Chem Phys*, 1982, 76, 3342-3343.
52. P. T. T. Wong and H. H. Mantsch, *Biochemistry*, 1985, 24, 4091-4096.
53. R. G. Snyder, S. L. Hsu and S. Krimm, *Spectrochim Acta A*, 1978, 34, 395-406.
54. B. P. Gaber, P. Yager and W. L. Peticolas, *Biophys J*, 1978, 21, 161-176.
55. M. R. Bunow and I. W. Levin, *Biochim Biophys Acta*, 1977, 487, 388-394.
56. H. Hamoudi, Z. Guo, M. Prato, C. Dablemont, W. Q. Zheng, B. Bourguignon, M. Canepa and V. A. Esaulov, *Phys Chem Chem Phys*, 2008, 10, 6836-6841.
57. J. A. Creighton, in *Spectroscopy of Surfaces*, John Wiley & Sons, New York, 1988.
58. J. A. Olmos-Asar, A. Rapallo and M. M. Mariscal, *Phys Chem Chem Phys*, 2011, 13, 6500-6506.
59. M. A. Bryant and J. E. Pemberton, *J Am Chem Soc*, 1991, 113, 3629-3637.

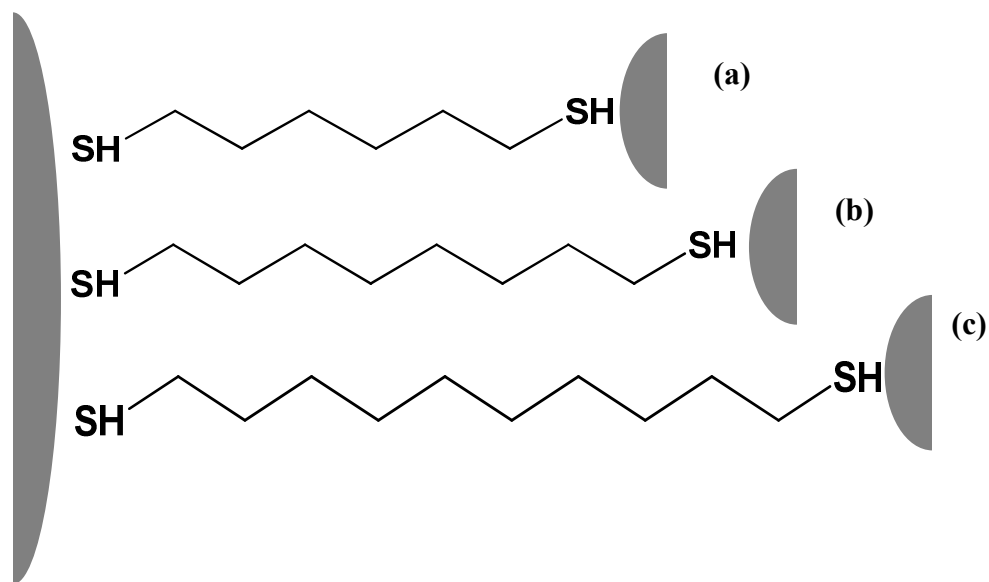


Figure 1. Structure of the studied aliphatic dithiols: a) 1,6-hexanedithiol (DT6), b) 1,8-octanedithiol (DT8), c) 1,10-decanedithiol (DT10) and model of NPs linkage through assembly of metal surfaces with both thiol groups leading to nanogaps of variable length.

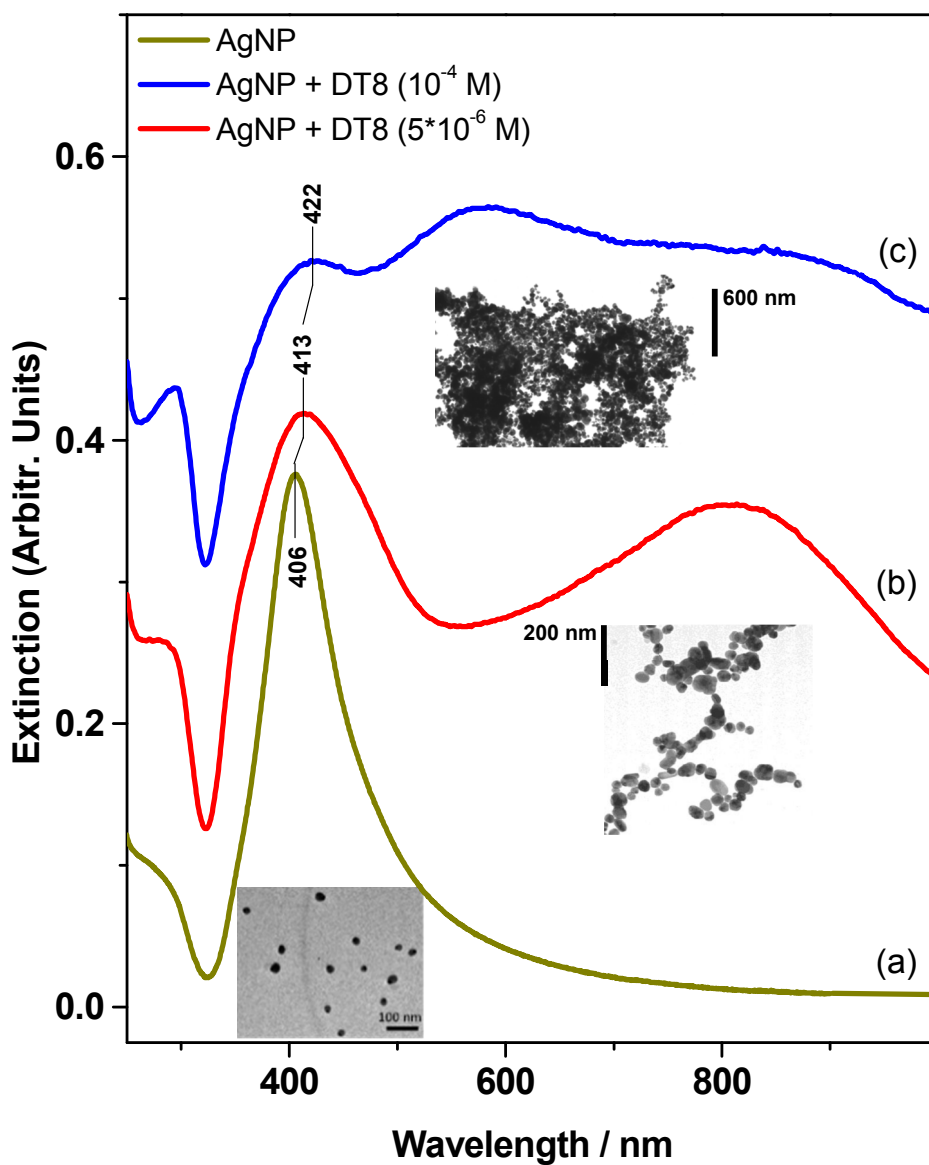


Figure 2. Extinction spectra of AgH nanoparticles in the absence (a) and in the presence of DT8 at 5×10^{-6} (b) and 10^{-4} M (c). In the inset TEM images the structure of isolated (a) and aggregated (b,c) NPs are shown.

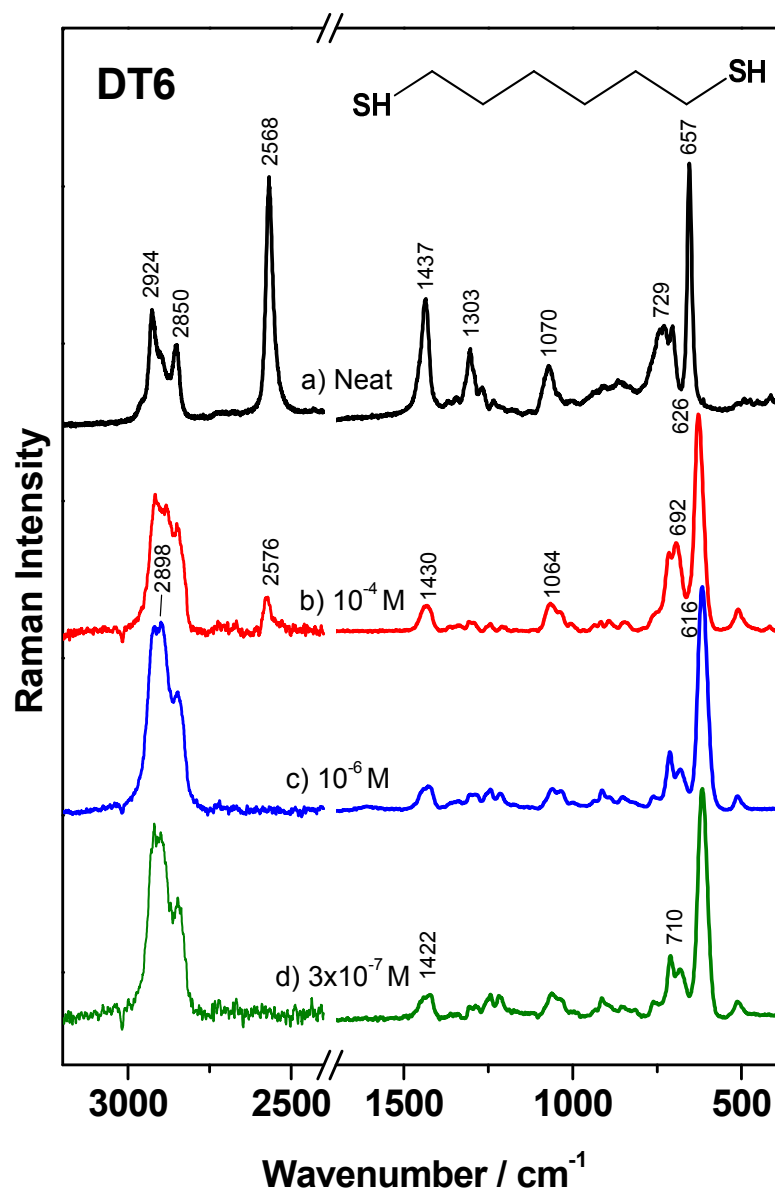


Figure 3. Raman spectrum of neat liquid DT6 (a) and SERS spectra of this dithiol on AgH at different concentrations: b) 10^{-4} ; c) 10^{-6} and d) 3×10^{-7} M. All spectra were obtained by using the 785 nm excitation line.

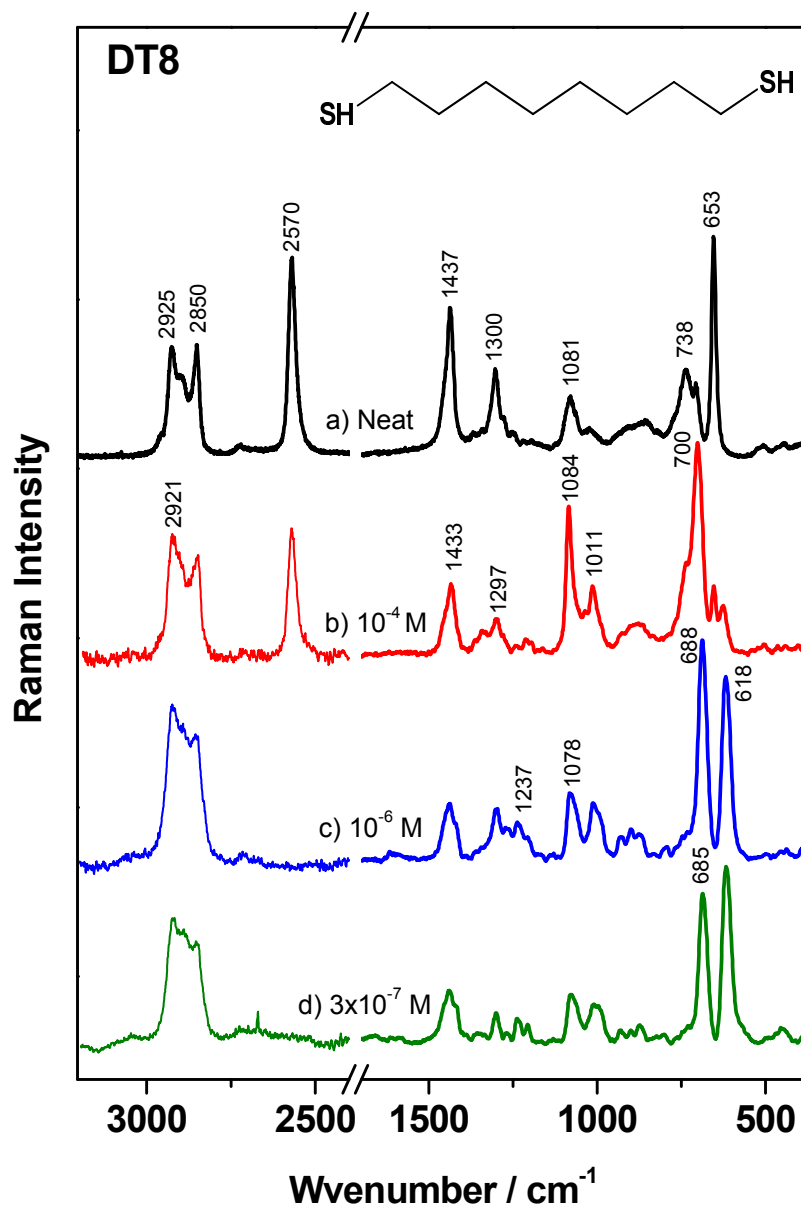


Figure 4. Raman spectrum of neat liquid DT8 (a) and SERS spectra of this dithiol on AgH at different concentrations: b) 10^{-4} ; c) 10^{-6} and d) 3×10^{-7} M. All spectra were obtained by using the 785 nm excitation line.

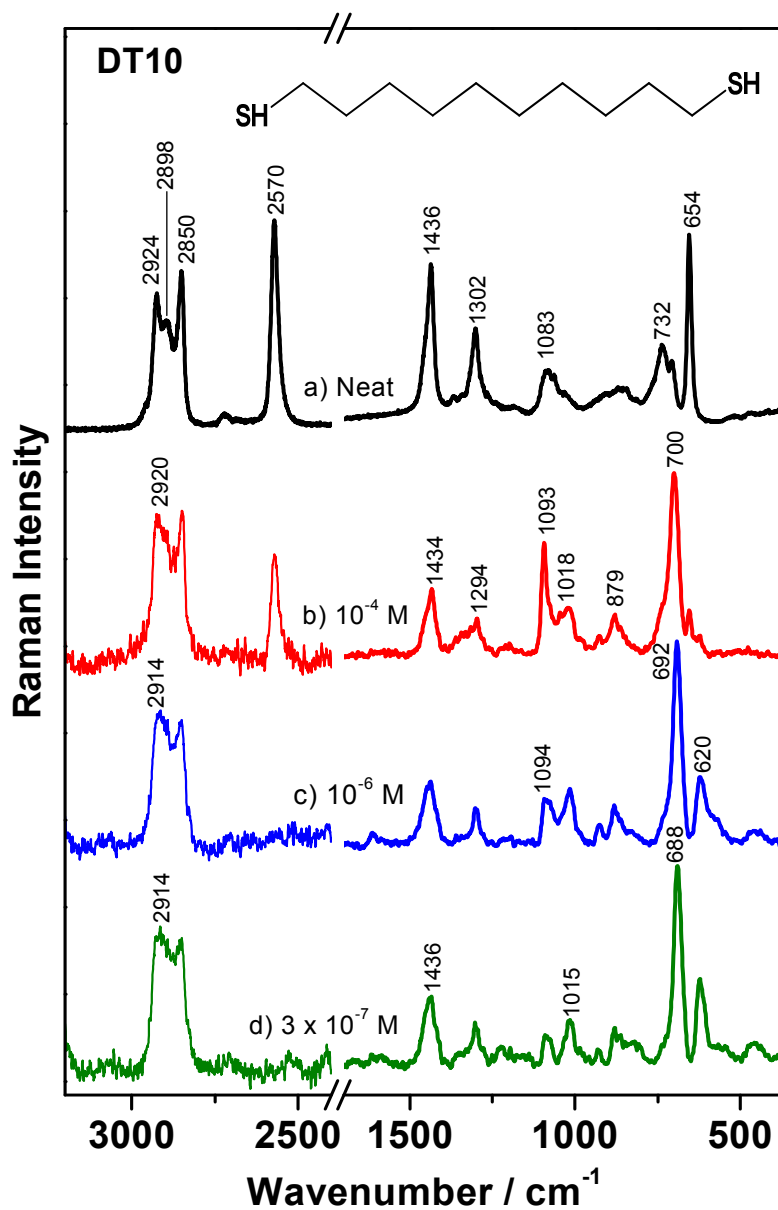


Figure 5. Raman spectrum of neat liquid DT10 (8) (a) and SERS spectra of this dithiol on AgH at different concentrations: b) 10⁻⁴ ; c) 10⁻⁶ and d) 3 x 10⁻⁷ M. All spectra were obtained by using the 785 nm excitation line.

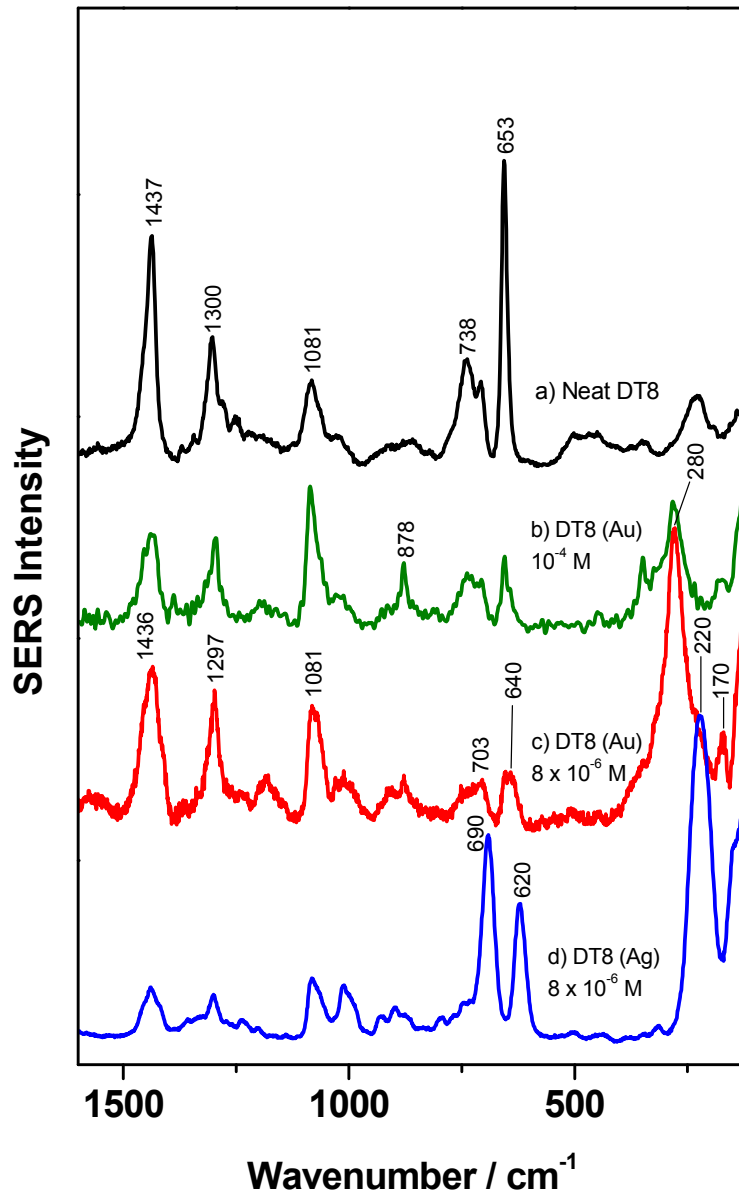


Figure 6. SERS of DT8 on AuC and AgH: (a) Raman spectrum of neat liquid DT8; (b) SERS spectrum of DT8 (8×10^{-6} M) on AuC; (c) SERS spectrum of DT8 (10^{-4} M) on AuC; and (d) SERS spectrum of DT8 (8×10^{-6} M) on AgH at. All spectra were obtained by using the 785 nm excitation line.

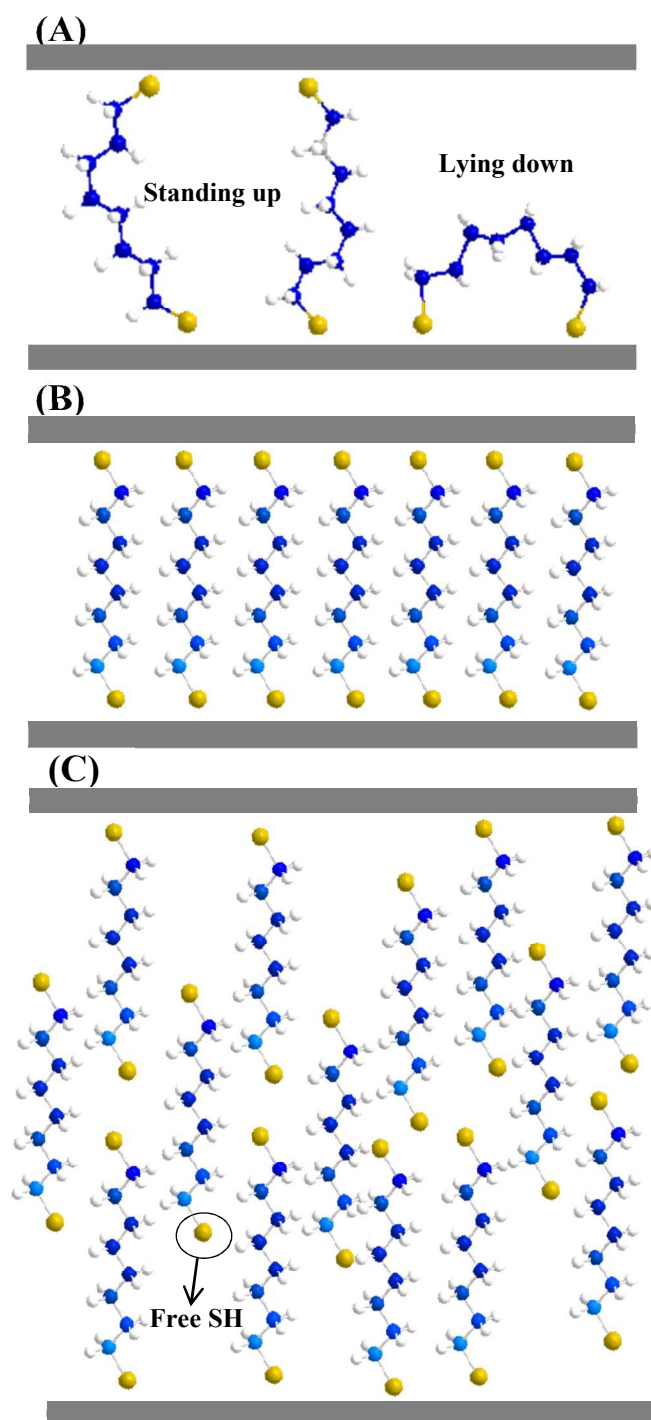


Figure 7. Different adsorption configurations deduced for DTX (specifically DT8) in nanogaps between two NPs at low surface coverage (A), where two possible adsorption patterns are possible (standing-up and lying-down); at conditions of self-assembled monolayer (SAM) (B), and at high metal surface coverage giving rise to the formation of multilayers (C), where free SH groups appear. The last configuration appears above a threshold concentration of $1\mu\text{M}$.

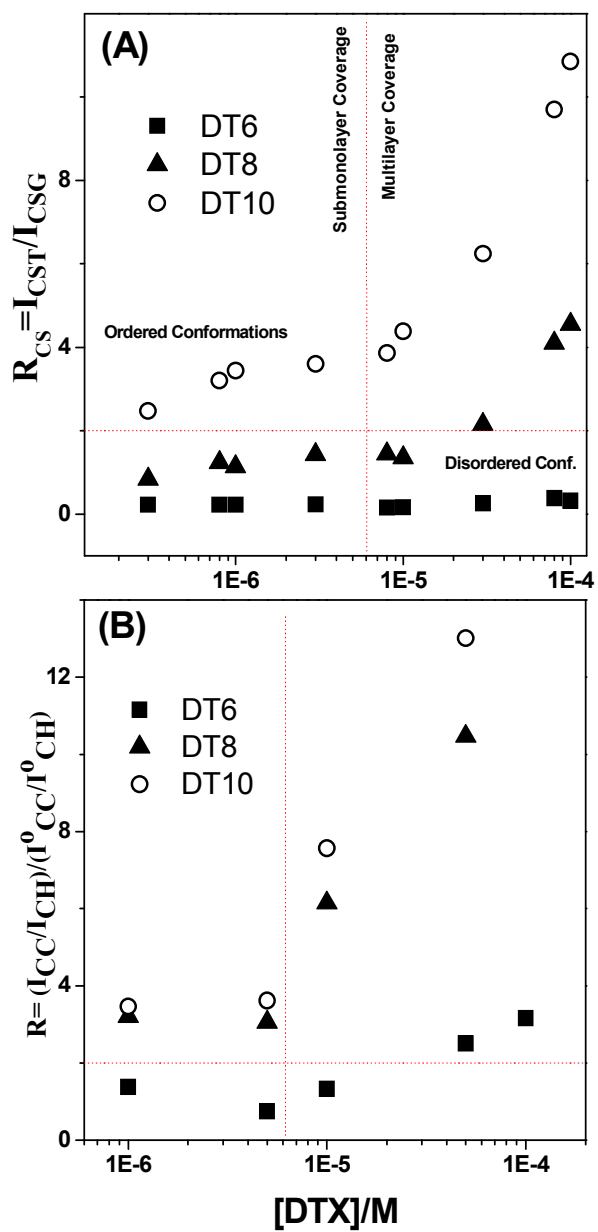


Figure 8. Plot of the $R_{CS} = I_{CST} / I_{CSG}$ (A) and $R = (I_{CC} / I_{CH}) / (I^0_{CC} / I^0_{CH})$ (B) ratios as a function of the dithiol concentration.

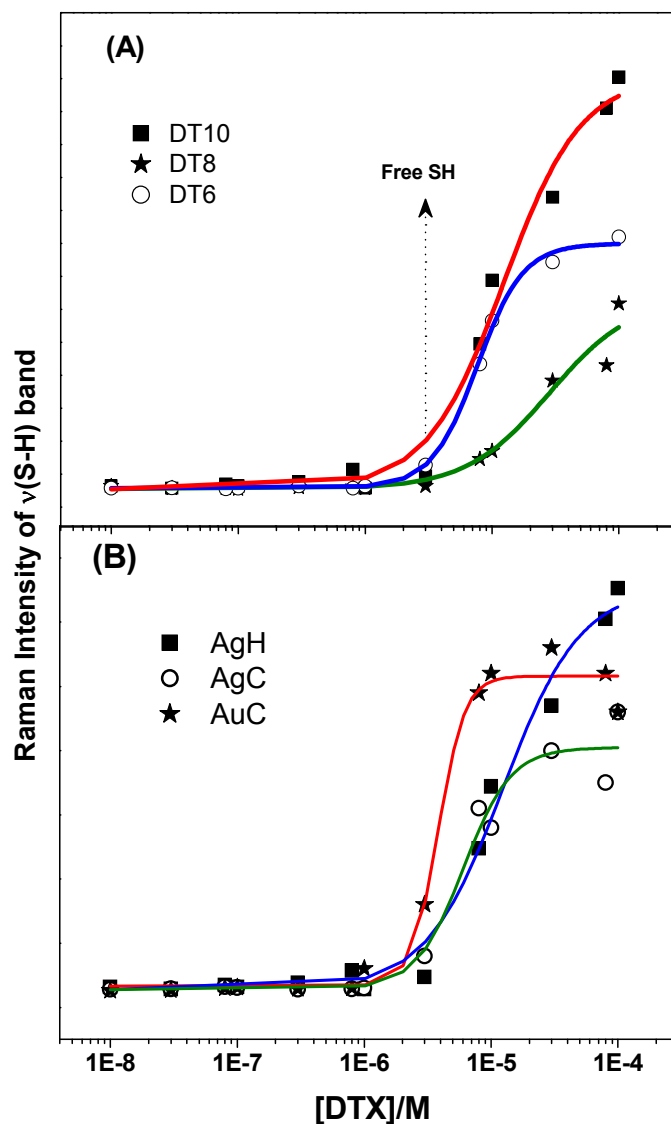


Figure 9. (A) Intensity of the free SH band (I_{SH}) determined from the SERS spectra of DT6, DT8 and DT10 on AgH colloid at different concentrations and normalized to the CH bands of the corresponding dithiol. (B) Intensity of the free $\nu(\text{SH})$ band corresponding to DT8 at different concentrations and using different SERS substrates.

Graphical Abstract

